Synthesis and Crystal Structure of $Ba_2Ti_{13}O_{22}$: A Reduced Form of $BaTi_5O_{11}$ by the Titanium Insertion

J. Akimoto,[1] Y. Gotoh, M. Sohma, K. Kawaguchi, and Y. Oosawa

National Institute of Materials and Chemical Research, Higashi, Tsukuba, Ibaraki 305, Japan

A new member of barium titanate compounds $Ba_2Ti_{13}O_{22}$ was synthesized by the reaction of $BaTiO_3$, Ti_2O_3, and TiO at 1853 K in an argon atmosphere. It crystallizes in the orthorhombic system, space group *Bmab*, $a = 11.6550(8)$ Å, $b = 14.1062(8)$ Å, $c = 10.0535(9)$ Å, $V = 1652.9(2)$ Å^3, and $Z = 4$. The structure was determined from a single-crystal X-ray diffraction study and refined to the conventional values of $R = 0.055$ and $wR = 0.043$ for 2050 observed reflections. The closest packing structure of Ba and O atoms in $Ba_2Ti_{13}O_{22}$ is identical with that in the $BaTi_5O_{11}$ structure. The vacant octahedral O_6 interstices in $BaTi_5O_{11}$ are completely occupied by the additional titanium cations in the present $Ba_2Ti_{13}O_{22}$, and the face-sharing Ti_2O_9 double group with a short Ti–Ti distance of 2.730(2) Å is formed as in the hexagonal $BaTiO_3$ structure. © 1994 Academic Press, Inc.

INTRODUCTION

The reduced titanium oxides form a class of compounds that can exhibit interesting electronic and magnetic properties such as $LiTi_2O_4$ of an oxide superconductor (1) and a semiconductor–metal transition in Ti_2O_3 (2), as well as their intriguing structural features. Recently single crystals of new reduced ternary titanates have been synthesized and their crystal structures have been determined; they are ramsdellite-type $Li_{0.5}TiO_2$ (3) in the Li–Ti–O system, calcium–ferrite-type $NaTi_2O_4$ (4), $Na_{2.08}Ti_4O_9$ (5), $Na_{1.7}Ti_6O_{11}$ (6), α-$NaFeO_2$-type $Na_{0.5}TiO_2$ (7), $Na_xTi_2O_4$ with $0.50 < x < 0.57$ (8), and $NaTi_8O_{13}$ (9) in the Na–Ti–O system, $SrTi_{11}O_{20}$ (10) in the Sr–Ti–O system, hollandite-type $La_{1.33}Ti_8O_{16}$ (10) in the La–Ti–O system, and $Nd_3Ti_4O_{12}$ (11) in the Nd–Ti–O system.

In the Ba–Ti–O system, three reduced compounds have been previously reported; hexagonal $BaTiO_{2.977}$ (12), $Ba_2Ti_6O_{13}$ (13), and hollandite-type $Ba_xTi_8O_{16}$ with $x = 1$ (14), and $x = 1.07$ and 1.31 (15). The average titanium valence states for these compounds, estimated by chemical formulae, lie between 3.67 and 3.95, in $Ba_2Ti_6O_{13}$ and $BaTiO_{2.977}$, respectively, and the compounds having only

[1] To whom correspondence should be addressed.

Ti^{3+} are not known yet in this system. We have examined the system BaO–Ti_2O_3–TiO_2 so as to separate new crystals with lower valence states of titanium for determining the crystal structures as well as their physical properties. In this paper, we describe the synthesis, crystal structure, and magnetic susceptibility of a new orthorhombic phase having the chemical formula $Ba_2Ti_{13}O_{22}$.

EXPERIMENTAL

Sample Preparation

Starting materials were $BaCO_3$ (CP grade), TiO_2 (99.9%), and Ti metal (99.9%). $BaTiO_3$ powder was first prepared by firing $BaCO_3$ and TiO_2 in the correct proportion at 1073 K for 15 hr, at 1273 K for 3 days, and at 1373 K for 18 hr in air. The product was identified as tetragonal $BaTiO_3$ (JCPDS No. 5-626) by X-ray powder diffraction. TiO and Ti_2O_3 were prepared by sintering TiO_2 and Ti metal in the correct proportions at 1773 K in an argon gas flow for several hours.

A mixture of $BaTiO_3$, Ti_2O_3, and TiO in a 2:2:3 molar ratio was placed in a Mo crucible with a Mo-foil lid, heated in a resistance furnace at 1853 K in an argon gas flow for several hours, and slowly cooled to room temperature. Dark black–purple single crystal were obtained with dimensions up to $0.5 \times 0.5 \times 0.4$ mm^3, as shown in Fig. 1. Platelet colorless of hexagonal $BaTiO_3$, $1 \times 1 \times 0.1$ mm^3 in maximum size, were also prepared in the surface region (16). EDX analysis showed that the black–purple crystals were barium titanate and were free from Mo contamination from the crucible. A molar ratio of Ba/Ti was approximately between 1/6 and 1/7. The chemical formula of this compound determined by the present structure analysis is $Ba_2Ti_{13}O_{22}$.

The Ti/O ratio in the sample was determined by thermogravimetric oxidative weight gain in dry air. The powdered sample (27.17 mg) was heated to 1273 K and the weight gain was found to be 7.21 wt.%, which was very consistent with the calculated value (7.68 wt.%) assuming oxidation to Ba–Ti^{4+}–O compounds. The X-ray powder
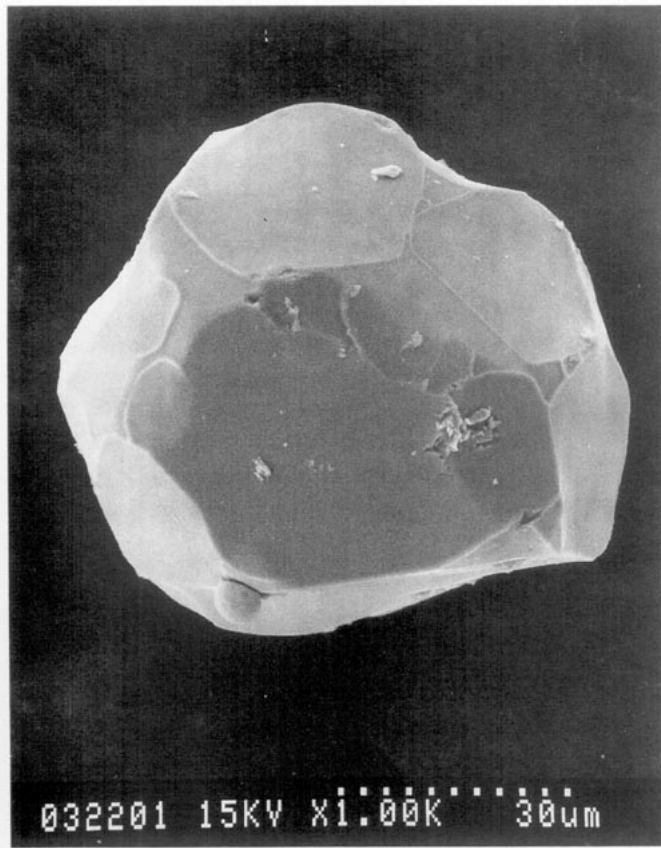
FIG. 1. SEM photograph of $Ba_2Ti_{13}O_{22}$ single crystal.

TABLE 1
X-Ray Powder Diffraction Data for $Ba_2Ti_{13}O_{22}$

h	k	l	$d_{calc}{}^a$ (Å)	d_{obs} (Å)	I/I_0
1	2	1	5.174	5.175	4
2	2	0	4.492	4.494	8
0	2	2	4.094	4.096	10
2	0	2	3.806	3.802	12
2	1	2	3.674	3.672	24
0	4	0	3.527	3.528 ⎫	32
3	1	1	3.509	3.512 ⎭	
0	3	2	3.434	3.432	9
2	2	2	3.349	3.346	14
3	2	1	3.222 ⎫		
1	4	1	3.200 ⎭	3.198	100
1	1	3	3.140	3.140	64
2	3	2	2.958	2.957	67
1	2	3	2.930	2.927	17
4	0	0	2.913	2.912	16
0	4	2	2.887	2.886	49
3	3	1	2.870	2.868	26
4	2	0	2.692	2.690	9
1	5	1	2.645	2.644	28
3	4	1	2.527 ⎫	2.528	19
4	0	2	2.520 ⎭		
3	1	3	2.497	2.497	32
4	1	2	2.481 ⎫	2.481	28
0	1	4	2.474 ⎭		
1	4	3	2.378	2.377	6
2	1	4	2.278	2.276	8
5	1	1	2.241	2.240	6
4	3	2	2.221 ⎫	2.221	61
0	3	4	2.217 ⎭		
2	6	0	2.180	2.179	9
0	6	2	2.130	2.130	10
2	3	4	2.072	2.072	19
4	4	2	2.050 ⎫	2.050	77
0	4	4	2.047 ⎬		
5	3	1	2.044 ⎭		
1	1	5	1.962	1.963	5
1	7	1	1.948	1.947	3
5	4	1	1.909 ⎫		
1	2	5	1.908 ⎭	1.907	12
5	1	3	1.896	1.895	5
4	5	2	1.880 ⎫		
0	5	4	1.877 ⎭	1.877	45
1	4	5	1.727	1.728	3
1	8	1	1.718 ⎫	1.718	17
0	6	4	1.717 ⎭		
6	3	2	1.690	1.691	5
0	0	6	1.676 ⎫		
4	4	4	1.675 ⎭	1.674	10
3	4	5	1.593	1.593	9
3	8	1	1.585	1.585	5
4	7	2	1.574 ⎫	1.575	36
0	7	4	1.572 ⎭		
3	5	5	1.509 ⎫	1.509	5
4	8	0	1.508 ⎭		
0	9	2	1.496	1.496	13
7	4	1	1.489 ⎫	1.489	4
5	2	5	1.488 ⎭		
7	1	3	1.482	1.483	9

pattern of the oxidized product was indexed to $BaTi_5O_{11}$ (JCPDS No. 35-805) and rutile-type TiO_2 (JCPDS No. 21-1276). From this result, the chemical formula of the as-grown crystal was determined to be $Ba_2Ti_{13}O_{22.2}$, which was consistent with the result of the present structure analysis.

Precession photographs indicate that the crystal belongs to the orthorhombic system with the possible space group $Bmab$ or $B2_1ab$. Table 1 shows the X-ray powder diffraction data of $Ba_2Ti_{13}O_{22}$ obtained at a scan rate of $2°/min$ in 2θ using graphite-monochromatized $CuK\alpha$ radiation and a Si internal standard. The lattice parameters, determined by least-squares refinement using $MoK\alpha_1$ radiation ($\lambda = 0.70926$ Å) and 25 well-centered reflections in the range $50 \leq 2\theta \leq 70°$ measured on an automated Rigaku AFC-5 four-circle diffractometer at 294 K, are $a = 11.6550(8)$, $b = 14.1062(8)$, $c = 10.0535(9)$ Å, and $V = 1652.9(2)$ Å^3.

Magnetic susceptibility of $Ba_2Ti_{13}O_{22}$ was measured between 4.3 and 300 K using a SQUID magnetometer. As shown in Fig. 2, the molar susceptibility χ of $Ba_2Ti_{13}O_{22}$ was nearly temperature independent in the range of 80 to 300 K, which might be due to a Van Vleck paramagnetism

TABLE 1—*Continued*

h	k	l	$d_{calc}{}^a$ (Å)	d_{obs} (Å)	I/I_0
4	6	4	1.479	1.479	8
6	3	4	1.461	1.461	4
8	0	0	1.456	1.456	13
4	0	6	1.452	1.452	56
4	1	6	1.445 ⎫		
4	8	2	1.445 ⎬		15
0	8	4	1.444 ⎭	1.444	
7	5	1	1.419	1.419	5
5	4	5	1.398 ⎫		
1	2	7	1.397 ⎭	1.397	4
0	9	4	1.330	1.330	10
2	6	6	1.329	1.329	
3	8	5	1.255	1.255	5
0	3	8	1.214	1.214	4
2	2	8	1.210 ⎫	1.210	7
4	9	4	1.210 ⎭		

^{a} Refined cell parameters using powder data are $a = 11.651(1)$ Å, $b = 14.107(1)$ Å, $c = 10.054(1)$ Å, and $V = 1652.4(2)$ Å³.

TABLE 2

Crystallographic and Experimental Data of $Ba_2Ti_{13}O_{22}$

Space group	*Bmab* (No. 64)
a (Å)	11.6550(8)
b (Å)	14.1062(8)
c (Å)	10.0535(9)
V (Å³)	1652.9(2)
Z	4
$D_x (g/cm^3)$	5.022
μ for MoKα (mm⁻¹)	10.63
Crystal shape	Approximate sphere
Crystal diameter (mm)	0.064
Scan mode	$2\theta - \omega$
Scan width (°)	$1.0 + 0.5 \tan \theta$
Scan speed (°/min)	2.0
Maximum 2θ (°)	80
Independent reflections	2659
Observed reflections	2050 ($>3\sigma$)
Final R	0.055
Final wR	0.043

as observed in other reduced titanium oxides, e.g., Ti_5O_9 (17), $LiTiO_2$ (18), $Li_{0.5}TiO_2$ (19), and $SrTiO_{2.72}$ (20). A sharp upturn in χ was, however, observed below 80 K, which might be due to a localized electron paramagnetic center or a paramagnetic impurity.

Structure Determination

A small spherical crystal, 0.064 mm in diameter, was used for crystal structure determination. The intensity data up to $2\theta = 80°$ was collected by the $2\theta - \omega$ scan method with a scan rate of 2°/min at 294 K on the four-circle diffractometer (operating conditions: 40 kV, 30 mA) using graphite monochromatized MoKα radiation ($\lambda = 0.71069$ Å), and reduced to structure factors after due
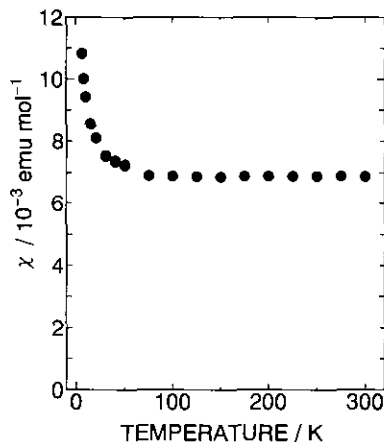

FIG. 2. Magnetic susceptibility of $Ba_2Ti_{13}O_{22}$ below room temperature.

corrections for absorption (using ACACA program (21)) and Lorentz and polarization effects. Fluctuations of the intensities, monitored by examining a set of the three standard reflections ((406), (054), (660)) taken after every 50 observations, were within 2.1%. A total of 2659 independent reflections were obtained, of which 2050 reflections have a criteria of $|F_{obs}| > 3\sigma(|F_{obs}|)$.

In the structure analysis that followed, the space group of highest symmetry, *Bmab*, confirmed by successful refinement, was adopted. Initial positions for one Ba, five Ti, and four O atoms were determined by the direct method using the computer program MULTAN80 system (22). The crystal structure factor F_{calc} was calculated with an overall temperature factor 0.47 by GSFFR program (23). The R value was 0.219, showing that the structure model was reasonable. Then the atomic parameters as well as scale and temperature factors were refined on F by the full-matrix least-squares refinement program RFINE2 (24) using 2050 unique reflections. The residual three oxygen atoms were located in the subsequent Fourier and difference Fourier syntheses. Final site occupation refinement for Ba and seven O sites confirmed the fully occupied model, which is consistent with the TGA result. Refinement with anisotropic thermal parameters and an isotropic secondary-extinction parameter ($g = 0.512(16) \times 10^{-4}$) gave final $R = 0.055$, $wR = 0.043$ [$w = 1/\sigma^2(F_{obs})$], with shift/error for all the parameters less than 0.01.

The scattering factors for neutral Ba, Ti, and O atoms tabulated by Cromer and Mann (25) were used in the calculations. The anomalous dispersion correction factors were taken from "International Tables X-Ray Crystallography" (26). The experimental and crystallographic data are summarized in Table 2. The final atomic coordi-

TABLE 3
Atomic Coordinates and Equivalent Isotropic Thermal Parameters for $Ba_2Ti_{13}O_{22}$

Atom	Position	x	y	z	B_{eq}
Ba	8f	0	0.08751(4)	0.33036(6)	0.84
Ti(1)	8f	0	0.33397(10)	0.16649(15)	0.53
Ti(2)	4a	0	0	0	0.54
Ti(3)	16g	0.25162(10)	0.15325(7)	0.17625(11)	0.73
Ti(4)	8d	0.25898(13)	0	0	0.54
Ti(5)	16g	0.12956(9)	0.32378(7)	0.42922(10)	0.56
O(1)	16g	0.2495(4)	0.4090(3)	0.3525(4)	0.69
O(2)	8f	0	0.2528(5)	0.0032(6)	0.61
O(3)	8e	0.25	0.25	0.0233(6)	0.60
O(4)	16g	0.1259(4)	0.0797(3)	0.0855(4)	0.57
O(5)	8f	0	0.4037(4)	0.3434(6)	0.56
O(6)	16g	0.1277(3)	0.2529(3)	0.2534(4)	0.53
O(7)	16g	0.1203(4)	0.4211(3)	0.0930(4)	0.70

TABLE 4
Selected Interatomic Bond Distances (Å) for $Ba_2Ti_{13}O_{22}$

Ba–O(1)	2.928(5) × 2	Ti(3)–O(1)	1.978(4)
O(2)	2.845(6)	O(4)	2.014(4)
O(4)	2.868(4) × 2	O(6)	2.159(4)
O(5)	3.126(6)	O(3)	2.056(4)
O(6)	2.874(4) × 2	O(6)	2.081(4)
O(7)	2.992(4) × 2	O(7)	2.007(4)
O(7)	2.841(4) × 2		
		Mean	2.049
Mean	2.915		
		Tl(4)–O(4)	2.100(4) × 4
Ti(1)–O(6)	2.070(4) × 2	O(1)	1.964(4) × 2
O(2)	2.002(6)	O(7)	2.023(4) × 2
O(5)	2.033(6)		
O(7)	2.006(4) × 2	Mean	2.029
Mean	2.031		
		Ti(5)–O(2)	1.999(4)
		O(6)	2.031(4)
Ti(2)–O(4)	2.039(4) × 4	O(1)	1.998(4)
O(5)	2.079(6) × 2	O(5)	2.073(4)
		O(3)	1.987(3)
Mean	2.052	O(4)	2.079(4)
		Mean	2.028
Ti(1)–Ti(3)	2.902(1) × 2	Ti(4)–Ti(2)	3.018(2)
Ti(5)	3.046(2) × 2	Ti(3)	2.796(1) × 2
		Ti(5)	2.993(1) × 2
Ti(2)–Ti(4)	3.018(2) × 2		
Ti(5)	2.994(1) × 4	Ti(5)–Ti(1)	3.046(2)
		Ti(2)	2.994(1)
Ti(3)–Ti(1)	2.902(1)	Ti(3)	2.880(2)
Ti(3)	2.730(2)	Ti(3)	2.914(2)
Ti(4)	2.796(1)	Ti(4)	2.993(1)
Ti(5)	2.880(2)	Ti(5)	3.020(2)
Ti(5)	2.914(2)		

nates and equivalent isotropic temperature factors are given in Table 3. Selected interatomic distances calculated using the UMBADTEA program (27) are listed in Table 4.

DESCRIPTION AND DISCUSSION OF THE STRUCTURE

The crystal structures of most barium titanates, i.e., hexagonal $BaTiO_3$ (16, 28), $Ba_6Ti_{17}O_{40}$ (29), $Ba_4Ti_{13}O_{30}$ (30), $Ba_2Ti_9O_{20}$ (31), $BaTi_5O_{11}$ (32), and $BaTi_6O_{13}$ (33), can be described as hexagonal closest packings consisting of Ba and O atoms and of vacancies between them (34). These structures can be illustrated as being made up of hexagonal closest packed layers with 4–6–8–10 layers per unit cell (35).

The crystal structure of the present $Ba_2Ti_{13}O_{22}$ belongs to the similar 6-layer group, which has the stacking sequence ABCACB or $(hcc)_2$ along the b-axis direction (Fig. 3). The stacking sequence of the oxygen O_8 layers (Y) and the barium-containing BaO_7 layers (Z) is $[YZZ]_\infty$, and the average thickness of the closest-packed layer is 2.35 Å, which corresponds to one-sixth of the b-axis length (14.1062 Å). This value is very consistent with the data of some barium titanates after Tillmanns et al. (34).

Figure 4 shows the idealized closest-packed Ba-containing layers in the compounds having the packing sequence ABCACB and the chemical formula $Ba_xM_yO_{11x}$, i.e., the present $Ba_2Ti_{13}O_{22}$ ($x = 2$, $y = 13$), $BaTi_5O_{11}$ ($x = 1$, $y = 5$) (32), $Ba_2Ti_{9.25}Li_3O_{22}$ ($x = 2$, $y = 12.25$) (37), and $BaZn_2Ti_4O_{11}$ ($x = 1$, $y = 6$) (35). Interestingly, the arrangement of Ba and O atoms in $Ba_2Ti_{13}O_{22}$ is identical with that in $BaTi_5O_{11}$, and further, the occupations of titanium cations in $BaTi_5O_{11}$ to the octahedral O_6 interstices are identical with parts of those in $Ba_2Ti_{13}O_{22}$. Namely, in the unit cell of $BaTi_5O_{11}$, 4 Ba and 44 O atoms

occupy in terms of a closest packing array. This packing produces the 26 octahedral O_6 interstices, as indicated by Tillmanns et al. (34), in which, 20 octahedral sites are occupied by titanium cations in $BaTi_5O_{11}$. Similarly, 4 Ba and 44 O atoms occupy in the half of the unit cell of $Ba_2Ti_{13}O_{22}$. However, the 26 octahedral O_6 interstices produced are completely occupied by titanium cations in $Ba_2Ti_{13}O_{22}$. An idealized BaO_7 layer ($y \sim 1/6$) is drawn in Fig. 5, indicating the occupations of titanium cations and the unit cells of both $BaTi_5O_{11}$ and $Ba_2Ti_{13}O_{22}$. The real monoclinic cell parameters of $BaTi_5O_{11}$ are $a = 7.6691(4)$ Å, $b = 14.0410(8)$ Å, $c = 7.5335(5)$ Å, and $\beta = 98.359(5)°$ (32), and the orthorhombic unit cell of the present $Ba_2Ti_{13}O_{22}$ can be transformed into the monoclinic cell ($a = 7.696$ Å, $b = 14.1062$ Å, $c = 7.696$ Å, and $\beta = 98.44°$) by the transformation matrix
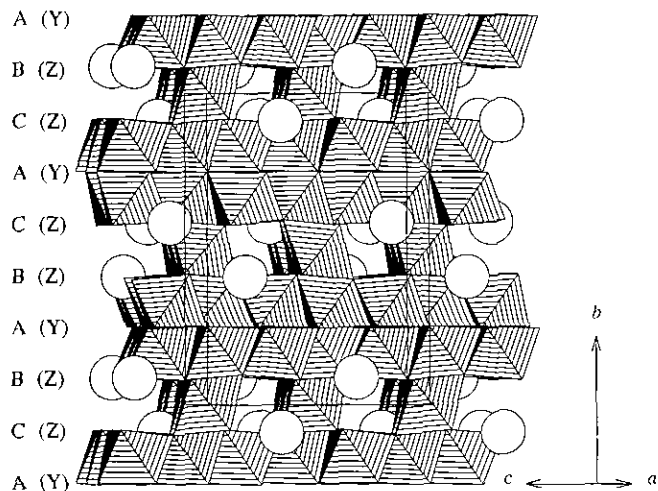
FIG. 3. Crystal structure of $Ba_2Ti_{13}O_{22}$ viewed along [100], drawn with STRUPLO90 (36).

FIG. 5. An idealized closest-packed BaO_7 layer ($y \sim 1/6$) and titanium cations of the above layer in $Ba_2Ti_{13}O_{22}$ and $BaTi_5O_{11}$. The closed small circles represent titanium cations occupied in both compounds and the open small circles represent those occupied only in $Ba_2Ti_{13}O_{22}$. The outlines of both unit cells are also indicated.

$$[1/2\ 0\ -1/2\ /\ 0\ 1\ 0\ /\ 1/2\ 0\ -1/2].$$

The crystal structures of $Ba_2Ti_{13}O_{22}$ and $BaTi_5O_{11}$ are shown in Figs. 6 and 7, respectively, at the six Ti levels in the unit cells. The vacant O_6 octahedron in $BaTi_5O_{11}$ is drawn as an octahedron without hatching. The titanium insertion to the $BaTi_5O_{11}$ structure produced the face-sharing Ti_2O_9 double group in the present $Ba_2Ti_{13}O_{22}$. The face-sharing $Ti(3)O_6$ octahedra are indicated by fully hatching in Fig. 6. Similar face-sharing double groups often can be seen in some barium titanate compounds or the lower valency titanium oxides, e.g., hexagonal $BaTiO_3$ (16), $Ba_6Ti_{17}O_{40}$ (29), Ti_2O_3 (38), and Ti_nO_{2n-1} (n = 4, 5, 6, 7, 8, 9) (39, 17, 40). The Ti(3)–Ti(3) distance across the shared O_3 face in $Ba_2Ti_{13}O_{22}$ is 2.730(2) Å, which is very short for the Ti–Ti distance, but is normal for the face-sharing octahedral environments in the above-mentioned titanates, 2.690 Å in hexagonal $BaTiO_3$ (16), 2.579 Å in Ti_2O_3 (38), and 2.811 Å in Ti_4O_7 (39).

In the $Ba_2Ti_{13}O_{22}$ structure, a linear 3 octahedral group and a condensed 5 octahedral group, which are formed by edge sharing, are observed in Figs. 6a and 6d and in Figs. 6b, 6c, 6e, and 6f, respectively. They are the basic units consisting of each stacking layer, and the 5 octahedral units are further condensed by sharing edges, giving face-sharing Ti_2O_9 double groups above and below layers. In the crystal structure of $Ba_4Ti_{13}O_{30}$ (30), as shown in Fig. 8, two similar kinds of octahedral units consist of each stacking layer. However, the 5 octahedral units are separated by Ba ions and are not connected by octahedral sharing each other in the stacking layer. As a result, face-sharing octahedral groups could not be observed in $Ba_4Ti_{13}O_{30}$.

The barium ion in $Ba_2Ti_{13}O_{22}$ is surrounded by twelve oxygen ions in a cuboctahedron where the Ba–O distances range from 2.841(4) to 3.126(6) Å, which give an average value of 2.915 Å. This coordination type is normal for barium atoms.
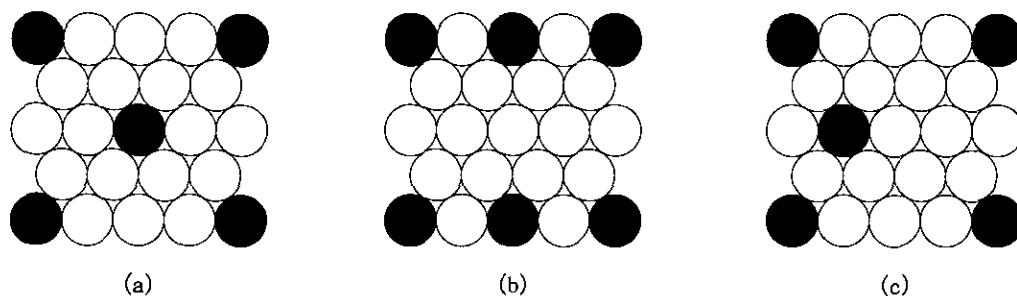
The individual Ti–O distance in $Ba_2Ti_{13}O_{22}$ varies in a

FIG. 4. Idealized closest-packed Ba-containing layers in the compounds having the packing sequence ABCACB, $[YZZ]_\infty$, and a general formula $Ba_xM_yO_{11x}$, (a) $Ba_2Ti_{13}O_{22}$ and $BaTi_5O_{11}$, (b) $Ba_2Ti_{9.25}Li_3O_{22}$, and (c) $BaZn_2Ti_4O_{11}$. The filled circles represent Ba atoms, and the open circles represent oxygen atoms, respectively.

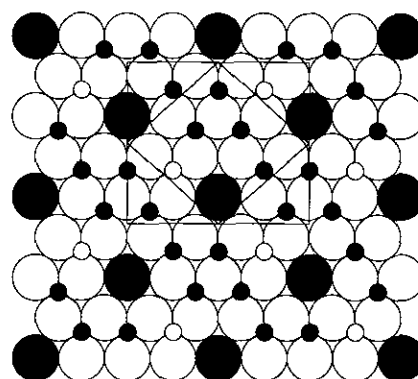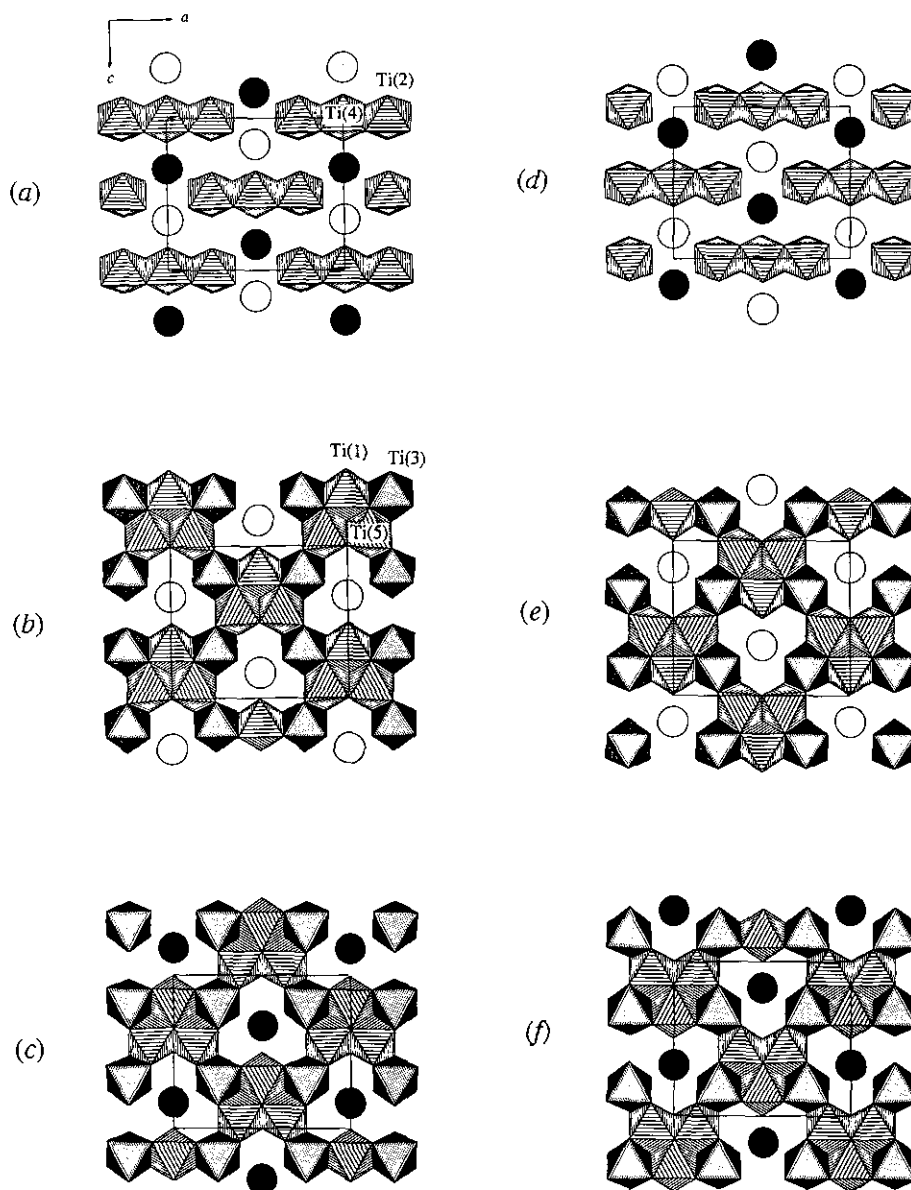FIG. 6.   Crystal structure of $Ba_2Ti_{13}O_{22}$ at the six Ti levels in the unit cell. (a) $y \sim 0$, (b) $y \sim 1/6$, (c) $y \sim 2/6$, (d) $y \sim 3/6$, (e) $y \sim 4/6$, and (f) $y \sim 5/6$ layers. The face-sharing $Ti(3)O_6$ octahedra are indicated by dark hatching. The closed and open circles represent Ba atoms at the oxygen levels above and below Ti atoms, respectively.

short range between 1.964(4) and 2.159(4) Å for Ti(4)–O(1) and Ti(3)–O(6) distances, respectively. The average octahedral Ti–O distances are 2.031 Å for Ti(1), 2.052 Å for Ti(2), 2.049 Å for Ti(3), 2.029 Å for Ti(4), and 2.028 Å for Ti(5), respectively (Table 4). The differences among them are within 0.024 Å, which is smaller than the difference of the effective ionic radii, 0.065 Å, between Ti^{3+} (0.670 Å) and Ti^{4+} (0.605 Å) tabulated by Shannon (41). This fact suggests that all Ti sites are randomly occupied by Ti^{3+} and Ti^{4+} cations. The mean Ti–O distance in $Ba_2Ti_{13}O_{22}$ is 2.037 Å, which is similar to the average Ti^{3+}–O distance of 2.048 Å in Ti_2O_3 (38).

CONCLUSION

We have succeeded in the synthesis of $Ba_2Ti_{13}O_{22}$ single crystals by the reaction of $BaTiO_3$, Ti_2O_3, and TiO at high temperatures. Magnetic susceptibility data below room temperature show a temperature-independent Pauli paramagnetism between 80 and 300 K. From the result of X-ray structure analysis, $Ba_2Ti_{13}O_{22}$ can be described as a reduced form of $BaTi_5O_{11}$ by the additional titanium cation insertion at the high temperature. Namely, the vacant octahedral O_6 interstices in $BaTi_5O_{11}$ are completely occu-
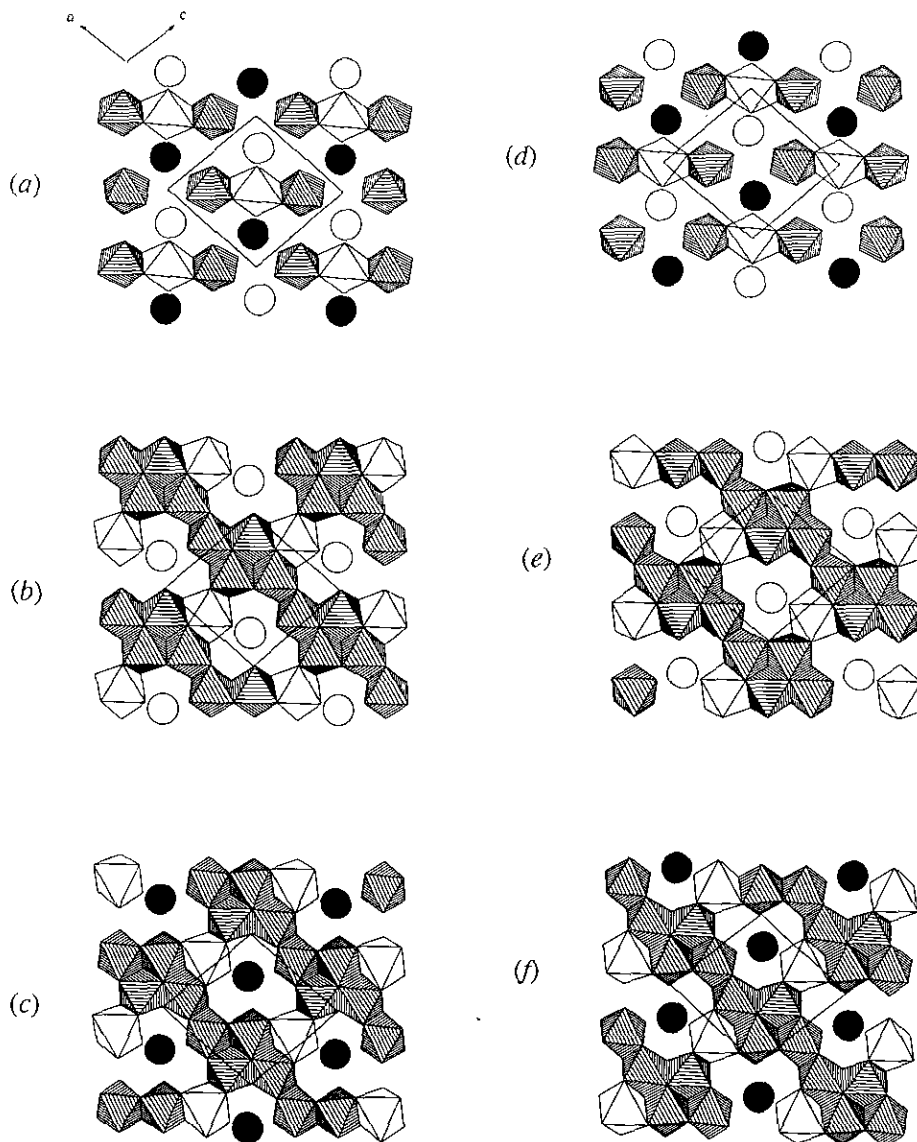
FIG. 7. Crystal structure of $BaTi_5O_{11}$ at the six Ti levels in the unit cell, after Tillmanns (32). (a) $y \sim 0$, (b) $y \sim 1/6$, (c) $y \sim 2/6$, (d) $y \sim 3/6$, (e) $y \sim 4/6$, and (f) $y \sim 5/6$ layers. The vacant O_6 octahedra are drawn as octahedra without hatching.

pied by titanium cations in the present $Ba_2Ti_{13}O_{22}$, resulting in the face-shared Ti_2O_9 double groups.

It is very interesting that the oxidized products of $Ba_2Ti_{13}O_{22}$ at 1273 K in the present TGA experiments are a mixture of $BaTi_5O_{11}$ and TiO_2, though $BaTi_5O_{11}$ is stable at low temperature (42, 43) and could not be prepared using the common solid-state ceramic techniques (43). This fact suggests the possibility of the topotactic oxidation or partly titanium cation extraction from the $Ba_2Ti_{13}O_{22}$ structure. Indeed, colorless single crystals have been synthesized by heating $Ba_2Ti_{13}O_{22}$ single-crystal specimens in an oxidation atmosphere below 1273 K. This oxidized "$BaTi_5O_{11}$" single crystal has a similar orthorhombic cell that remains unchanged, though weak superstructure spots of $k \neq 2n$ for $hk0$ reflections are

observed by X-ray precession method. The refined cell parameters on the four-circle diffractometer are $a = 11.619(2)$ Å, $b = 14.085(2)$ Å, and $c = 10.046(2)$ Å. The superstructure diffraction spots may indicate the existence and the ordering of the titanium site vacancy in the orthorhombic "$BaTi_5O_{11}$". Further experiments concerning chemical composition and titanium occupation of the "$BaTi_5O_{11}$" single crystal are now being carried out.

In the preparation of this paper, we encountered a paper concerning the synthesis and crystal structure of $Ba_2Ti_{12}^{3+}Ti^{4+}O_{22}$ (44). The framework structure and each site symmetry are identical with those in our results. However, some significant differences in the structural parameters can be seen. Their lattice parameters, which are $a = 11.575(5)$ Å, $b = 14.094(8)$ Å, and $c = 10.018(3)$ Å,
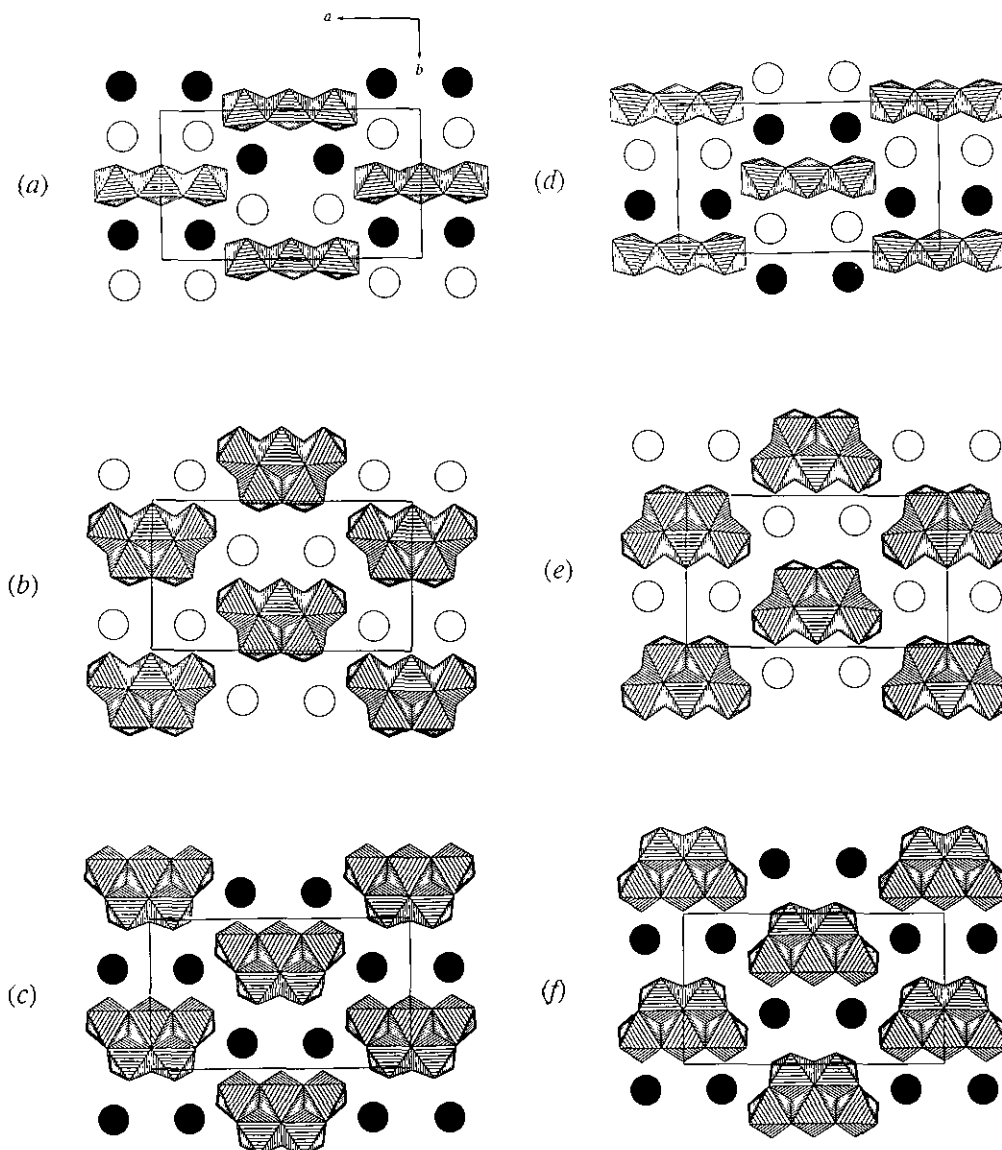
FIG. 8. Crystal structure of $Ba_4Ti_{13}O_{30}$ at the six Ti levels in the unit cell, after Tillmanns (30). (a) $z \sim 0$, (b) $z \sim 1/6$, (c) $z \sim 2/6$, (d) $z \sim 3/6$, (e) $z \sim 4/6$, and (f) $z \sim 5/6$ layers.

are much smaller than the present values of $a = 11.6550(8)$ Å, $b = 14.1062(8)$ Å, and $c = 10.0535(9)$ Å, and are similar to those of our oxidized one. Moreover, the Ba–O cuboctahedron and all of the Ti–O octahedra are more distorted than those in our results. These differences may be caused by the different synthetic procedure.

REFERENCES

1. D. C. Johnston, *J. Low Temp. Phys.* **25**, 145 (1976).
2. C. E. Rice and W. R. Robinson, *Mater. Res. Bull.* **11**, 1355 (1976).
3. J. Akimoto, Y. Gotoh, M. Sohma, K. Kawaguchi, Y. Oosawa, and H. Takei, *J. Solid State Chem.*, **110**, 150 (1994).
4. J. Akimoto and H. Takei, *J. Solid State Chem.* **79**, 212 (1989).
5. J. Akimoto and H. Takei, *J. Solid State Chem.* **83**, 132 (1989).
6. J. Akimoto and H. Takei, *J. Solid State Chem.* **85**, 8 (1990).
7. J. Akimoto and H. Takei, *J. Solid State Chem.* **85**, 31 (1990).
8. J. Akimoto and H. Takei, *J. Solid State Chem.* **90**, 92 (1991).
9. J. Akimoto and H. Takei, *J. Solid State Chem.* **90**, 147 (1991).
10. B. Hessen, S. A. Sunshine, and T. Siegrist, *J. Solid State Chem.* **94**, 306 (1991).
11. B. Hessen, S. A. Sunshine, T. Siegrist, and R. B. Van Dover, *J. Solid State Chem.* **105**, 107 (1993).
12. H. Arend and L. Kihlborg, *J. Am. Ceram. Soc.* **52**, 63 (1969).
13. J. Schmachtel and Hk. Müller-Buschbaum, *Z. Anorg. Allg. Chem.* **435**, 243 (1977).
14. J. Schmachtel and Hk. Müller-Buschbaum, *Z. Naturforsch. B* **35**, 332 (1980).
15. R. W. Cheary, *Acta Crystallogr. Sect. B* **46**, 599 (1990).

16. J. Akimoto, Y. Gotoh, and Y. Oosawa, *Acta Crystallogr., Sect. C* **50**, 160 (1994).
17. M. Marezio, D. Tranqui, S. Lakkis, and C. Schlenker, *Phys. Rev. B* **16**, 2811 (1977).
18. T. A. Hewston and B. L. Chamberland, *J. Phys. Chem. Solids* **48**, 97 (1987).
19. J. Akimoto, Y. Gotoh, M. Sohma, K. Kawaguchi, Y. Oosawa, and H. Takei, *J. Solid State Chem.*, in press.
20. W. Gong, H. Yun, Y. B. Ning, J. E. Greedan, W. R. Datars, and C. V. Stager, *J. Solid State Chem.* **90**, 320 (1991).
21. B. J. Wuensch and C. T. Prewitt, *Z. Kristallogr.* **122**, 24 (1965).
22. H. F. Fan, J. X. Yao, P. Main, and M. M. Woolfson, *Acta Crystallogr., Sect. A* **39**, 566 (1983).
23. M. Ohmasa, "GSFFR: Patterson, Fourier, and Difference Fourier Syntheses Program," 1972.
24. L. W. Finger, "Carnegie Institution of Washington Year Book," Vol. 67, p. 216. Carnegie Institution of Washington, Washington, DC, 1969.
25. D. T. Cromer and J. B. Mann, *Acta Crystallogr. Sect.* **A24**, 321 (1968).
26. "International Tables for X-Ray Crystallography," Vol. IV, p. 148. Kynoch Press, Birmingham, 1974.
27. L. W. Finger and E. Prince, "National Bureau of Standards Technical Note," Vol. 854, p. 54, U.S. Government Printing Office, Washington, DC, 1975.
28. R. D. Burbank and H. T. Evans, Jr., *Acta Crystallogr.* **1**, 330 (1948).
29. W. Hofmeister, E. Tillmanns, and W. H. Baur, *Acta Crystallogr., Sect. C* **40**, 1510 (1984).
30. E. Tillmanns, *Cryst. Struct. Commun.* **11**, 2087 (1982).
31. E. Tillmanns, W. Hofmeister, and W. H. Baur, *J. Am. Ceram. Soc.* **66**, 268 (1983).
32. E. Tillmanns, *Acta Crystallogr.* **25**, 1444 (1969).
33. E. Tillmanns, *Cryst. Struct. Commun.* **1**, 1 (1972).
34. E. Tillmanns, W. Hofmeister, and W. H. Baur, *J. Solid State Chem.* **58**, 14 (1985).
35. R. S. Roth, C. J. Rawn, C. G. Lindsay, and W. Wong-Ng, *J. Solid State Chem.* **104**, 99 (1993).
36. R. X. Fischer, A le Lirzin, D. Kassner, and B. Rüdinger, *Z. Kristallogr. Suppl. Issue* **3**, 75 (1991).
37. E. Tillmans and I. Wendt, *Z. Kristallogr.* **144**, 16 (1976).
38. W. R. Robinson, *J. Solid State Chem.* **9**, 255 (1974).
39. M. Marezio, D. B. McWahn, P. D. Dernier, and J. P. Remeika, *J. Solid State Chem.* **6**, 213 (1973).
40. Y. le Page and P. Strobel, *J. Solid State Chem.* **44**, 273 (1982).
41. R. D. Shannon, *Acta Crystallogr.* **32**, 751 (1976).
42. P. K. Davies and R. S. Roth, *J. Solid State Chem.* **71**, 503 (1987).
43. J. J. Ritter, R. S. Roth, and J. E. Blendell, *J. Am. Ceram. Soc.* **69**, 155 (1986).
44. S. Möhr and Hk. Müller-Buschbaum, *J. Alloys and Compounds* **199**, 203 (1993).